

Data-Driven Falsification of Cyber-Physical Systems

Atanu Kundu, Sauvik Gon, Rajarshi Ray

Abstract—Cyber-Physical Systems (CPS) are abundant in safety-critical domains such as healthcare, avionics, and autonomous vehicles. Formal verification of their operational safety is, therefore, of utmost importance. In this paper, we address the falsification problem, where the focus is on searching for an unsafe execution in the system instead of proving their absence. The contribution of this paper is a framework that (a) connects the falsification of CPS with the falsification of deep neural networks (DNNs) and (b) leverages the inherent interpretability of Decision Trees for faster falsification of CPS. This is achieved by: (1) building a surrogate model of the CPS under test, either as a DNN model or a Decision Tree, (2) application of various DNN falsification tools to falsify CPS, and (3) a novel falsification algorithm guided by the explanations of safety violations of the CPS model extracted from its Decision Tree surrogate. The proposed framework has the potential to exploit a repertoire of *adversarial attack* algorithms designed to falsify robustness properties of DNNs, as well as state-of-the-art falsification algorithms for DNNs. Although the presented methodology is applicable to systems that can be executed/simulated in general, we demonstrate its effectiveness, particularly in CPS. We show that our framework implemented as a tool FLEXIFAL can detect hard-to-find counterexamples in CPS that have linear and non-linear dynamics. Decision tree-guided falsification shows promising results in efficiently finding multiple counterexamples in the ARCH-COMP 2024 falsification benchmarks [22].

Index Terms—Falsification, CPS, feedforward neural network, Decision Tree, Signal Temporal Logic.

I. INTRODUCTION

The traditional simulation and testing techniques can be effective for debugging the early stages of Cyber-Physical-Systems (CPS) design. However, as the design becomes pristine by passing through multiple phases of testing, finding the lurking bugs becomes computationally expensive and challenging by means of simulation and testing alone. Formal verification techniques such as model-checking come in handy here by either proving the absence of bugs in such designs or by providing a *counterexample* behavior that violates the specification. A complementary approach is *falsification*, where the focus is solely on discovering a system behavior that is a counterexample to a given specification. In this work, we address the falsification of safety specifications expressed in signal temporal logic [27] for CPS given as an executable.

Our Contribution The contribution of this paper is a falsification framework that employs two strategies. First, it connects the falsification of reachability specifications of CPS with the falsification of reachability specifications of deep neural networks (DNNs). Second, it leverages on the inherent interpretability of Decision Trees for faster falsification of signal

temporal logic (STL) specifications of CPS. This is achieved by: (1) building a surrogate model of the CPS under test, either as a DNN model or a Decision Tree, (2) application of various DNN falsification tools to falsify CPS, and (3) a falsification algorithm guided by the interpretations of safety violation of a CPS model extracted from its Decision Tree surrogate. The proposed framework has the potential to exploit a repertoire of *adversarial attack* algorithms designed to falsify the robustness properties of DNNs as well as state-of-the-art falsification algorithms designed for DNNs. A reachability specification of a CPS directly maps to a reachability specification of a DNN when the latter approximates the former. Furthermore, a recent work has shown that a reachability specification of a DNN can be reduced to an equivalent set of robustness specifications [33]. A robustness specification conveys that the network’s output on an ϵ -perturbed input matches with its output on the unperturbed version [8], [35], [40]. This reduction allows the use of adversarial attack algorithms in the literature of DNN [15], [25], [29], [26], which are targeted to falsify robustness specification, for falsification of CPS. Our framework provides an interface to several tools that can falsify the safety properties of DNNs as well as an interface to a variety of *adversarial attack* algorithms that are aimed towards the falsification of robustness specification of DNNs. These tools and algorithms have complementary strengths. As a result, there is a high likelihood of success in a falsification task when trying the various falsification tools and algorithms through the interface. A limitation of DNN-based falsification is the considerable computational resources it consumes to build a surrogate model from data and consequently to find a counterexample. To address this limitation, our framework integrates a falsification strategy based on building a decision tree as a surrogate model. A decision tree, in contrast to a DNN, is comparatively cheaper to build and its inherent explainability provides a mechanism for efficiently searching multiple counterexamples which we shall discuss in detail later in the paper. The primary challenge of this framework is to construct a faithful surrogate model of the CPS, which we carry out by generating traces from the CPS executable and learning (supervised) from the traces. For complex CPS such as highly autonomous vehicles, designing a faithful model such as a hybrid automaton [1] may not be practical due to complex dynamics. Furthermore, models combining explicit hybrid automaton and *black-box* executable may be relevant and practical for real-world CPS [12]. The proposed framework can be beneficial for falsifying these types of system, since it relies only on CPS trajectory data. Although the proposed falsification framework applies to executable systems in general, this work is focused on exploring its effectiveness in CPS in particular, and we report our findings. In summary, the main contributions of the paper are as follows.

A. Kundu and S. Gon are students of the Indian Association for the Cultivation of Science (IACS), India. Email: { mcsak2346, ugs2584 }@iacs.res.in. Dr. R. Ray is an Associate Professor at IACS, India. Email: rajarshi.ray@iacs.res.in

- A data-driven framework for falsification of CPS safety specifications given as an executable (black-box). A tool FLEXIFAL implementing the framework.
- A labeled dataset representing a number of CPS obtained from their executed/simulated trajectories. The dataset can be beneficial for building machine learning models for CPS analysis and is publicly available.¹
- Neural network surrogates of representative hybrid automata and Simulink models of CPS are made publicly available in onnx format.²

II. PRELIMINARIES

In this work, we use a fully connected feed-forward neural network with the rectified linear unit (*ReLU*) activation function, and a decision tree as the machine learning models to approximate a CPS. A neural network can be seen as computing a function $N : \mathbb{R}^{n_1} \rightarrow \mathbb{R}^{n_2}$, where n_1 and n_2 denotes the number of inputs and outputs of the network respectively. A decision tree is a supervised machine learning model for classification and regression tasks. In this work, we employ CART (Classification and Regression Tasks) among the several decision tree construction algorithms [6]. Safety requirements are often represented using *reachability specification*. A reachability specification comprises a set of initial configurations (\mathcal{I}) and a set of unsafe configurations (\mathcal{U}) of the system and specifies that for all inputs $x \in \mathcal{I}$, the output of the system does not belong to \mathcal{U} . The falsification problem of a reachability specification of a network is given as:

Definition 1 (Falsification of Reachability Specification): Given a deep neural network that computes the function $N : \mathbb{R}^{n_1} \rightarrow \mathbb{R}^{n_2}$ and a reachability specification $(\mathcal{I}, \mathcal{U})$ such that $\mathcal{I} \subseteq \mathbb{R}^{n_1}$ and $\mathcal{U} \subseteq \mathbb{R}^{n_2}$, the falsification problem is to find $x \in \mathcal{I}$ such that $N(x) \in \mathcal{U}$.

The robustness specification when applied to classification models refers to the network’s ability to keep its classification unchanged when its input is perturbed within an ϵ neighborhood. We formally define a local robustness specification of DNN as follows:

Definition 2 (Local Robustness Specification): Given a deep neural network that computes the function $N : \mathbb{R}^{n_1} \rightarrow \mathbb{R}^{n_2}$ and an input $x \in \mathbb{R}^{n_1}$, the network is said to be locally robust with respect to the input x if $N(x) = N(x')$ for all x' in the ϵ neighbourhood of input x .

The robustness of a network can be refuted by showing the presence of an ϵ -perturbed input for the given input x such that the network’s outcome on x and the perturbed version do not match.

In the text, we depict an n -dimensional deterministic CPS by a function $\mathcal{M} : \mathcal{P} \times \mathbb{C}(\mathbb{R}) \times \mathbb{R} \rightarrow \mathbb{R}^n$, where $\mathcal{P} \subseteq \mathbb{R}^n$ is the set of initial system configurations, $\mathbb{C}(\mathbb{R})$ is the space of continuous functions $u : \mathbb{R} \rightarrow \mathbb{R}^m$ representing a time-varying m -dimensional input signal to the CPS. An input signal is a function that maps a time instant t , to an input $u(t) \in \mathbb{R}^m$ to the CPS. The function $\mathcal{M}(x_0, u, t)$ represents the state that the CPS reaches, starting from the initial system configuration

x_0 , under the influence of the input signal u and running for t time units. In this work, we restrict ourselves to deterministic CPS. A CPS trajectory depicts how the variables in the system change over time. It can be formally defined as follows.

Definition 3: A trajectory of a CPS $\mathcal{M} : \mathcal{P} \times \mathbb{C}(\mathbb{R}) \times \mathbb{R} \rightarrow \mathbb{R}^n$, starting from an initial system configuration $x_0 \in \mathcal{P}$, with an input signal $u \in \mathbb{C}(\mathbb{R})$ over a time horizon T is given by a function $\Gamma : [0, T] \rightarrow \mathbb{R}^n$ such that for any $t_1, t_2 \in [0, T]$ where $t_1 < t_2$, $\Gamma(t_2) = \mathcal{M}(\Gamma(t_1), u, t_2 - t_1)$.

We now state a CPS’s falsification problem, which we address in Section III of the paper. A general falsification problem of STL specification is defined and addressed in Section IV.

Problem Statement 1: Given a CPS $\mathcal{M} : \mathcal{P} \times \mathbb{C}(\mathbb{R}) \times \mathbb{R} \rightarrow \mathbb{R}^n$ and a reachability specification $(\mathcal{I}, \mathcal{U})$ where $\mathcal{I} \subseteq \mathcal{P} \times \mathbb{C}(\mathbb{R}) \times \mathbb{R}$ and $\mathcal{U} \subseteq \mathbb{R}^n$, find a tuple $\mathcal{C} = (x_c, u_c, t_c)$, an element of \mathcal{I} with an initial system configuration x_c , an input signal u_c and a time t_c such that $\mathcal{M}(x_0, u_c, t_c) \cap \mathcal{U} \neq \emptyset$. Such a tuple is called a counterexample. In this work, we are limited to finding a counterexample having a piecewise-constant input signal, with equally spaced control points over time. Bounded ranges for each dimension of the input are assumed to be known.

III. FRAMEWORK FOR CPS FALSIFICATION

We now present our falsification framework FLEXIFAL, which consists of mainly two procedures, DNN-based falsification and falsification using a Decision Tree. This section focuses on describing the DNN-based falsification NNFAL, while the decision tree-based falsification procedure is described in the subsequent section. The foremost step is building a DNN model from the CPS (given as an executable) that we intend to falsify against a given reachability specification. This construction reduces the falsification problem of the CPS to the falsification of the constructed DNN. The next step is to search for a counterexample of the reachability specification in the constructed DNN either by using one of the DNN falsification tools or by using one of the adversarial attack algorithms to falsify local robustness specification. The relation between the falsification of a reachability specification and the falsification of the local robustness specification of DNN is shown in [33]. The last step of our algorithm is to validate whether the generated counterexample is spurious or real by execution on the actual CPS. If the execution lends the counterexample as spurious, we modify the reachability specification by adding necessary constraint(s) in order to exclude the spurious counterexample from the search space. The falsification tool is invoked with the modified specification of the DNN. The modified specification forbids the tool from repeatedly generating spurious counterexamples. The steps of invocation, validation, and specification modification of the falsification tool are repeated. The algorithm terminates on two conditions. The first condition is when a valid counterexample is found, declaring that the DNN, and thus the CPS is falsified. The other termination condition is due to a timeout before finding a valid counterexample, in which case, the algorithm terminates by declaring failure. Figure 1 depicts an overview of our proposed framework, and the block diagram of NNFAL is shown on the right. We now discuss the details of NNFAL.

¹Data sets of the CPS under test.

²Neural-network models of the corresponding CPS.

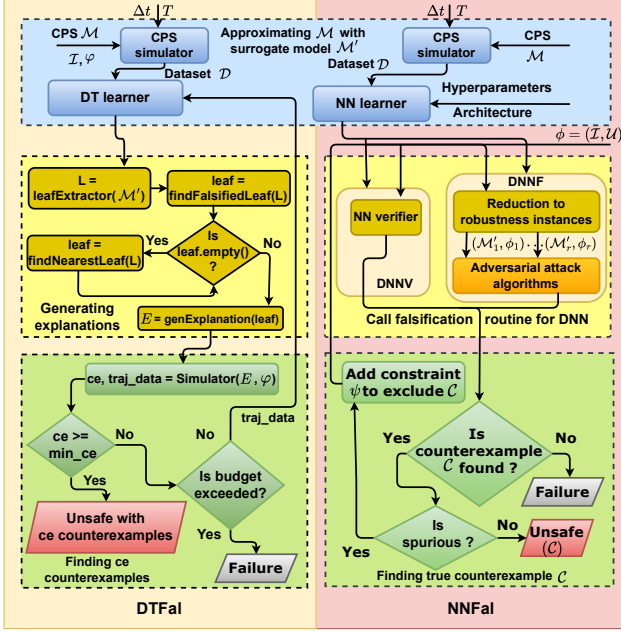


Fig. 1: The flowchart of the falsification framework FLEX-IFAL. The framework incorporates two distinct falsification strategies, DTFAL (left) and NNFal (right).

A. CPS design to Neural Networks

1) *Dataset Generation from CPS*: The primary step in constructing a neural network model from the CPS is building a labeled dataset. Since trajectories of a CPS represent its behavior, a machine learning model ought to be learned from trajectories. In this work, we consider models of CPS (Simulink/Hybrid automata) and then use model simulators (Matlab Simulink model simulator/ XSpeed hybrid automata simulator) to generate a dataset \mathcal{D} from a CPS \mathcal{M} . In this work, we use a model solely to generate simulated trajectories. The simulators use numerical ode solvers such as CVODE [32] to simulate continuous behaviors of the CPS. To formally describe the dataset, we use some notations as follows. We represent a time discretization of a trajectory of the CPS at Δt time-steps as $\Gamma(j\Delta t) = \mathcal{M}(x_0, u, j\Delta t)$. To represent the time-varying input signal $u(t)$ in the dataset, we consider k partitions of the time horizon and consider a fixed input in each interval. This scheme discretizes the time-varying input into a piece-wise constant input, which can be represented as an element of $\mathbb{R}^{k \times m}$. The larger the partitions k , the closer the data representation becomes to the actual time-varying input. However, increased partitions increase the parameters in the dataset and hence the data size. In this work, we determinize the *may* transition semantics and the mode-switching updates. To determinize the *may* transition semantics, we generate our data with urgent transition semantics in the CPS simulator, which means a transition is taken as soon as its guard is enabled. To address the uncertainty in the state updates, we remove non-deterministic choices in the CPS across all simulations. Algorithm 1 depicts the generation of the dataset \mathcal{D} for N simulated trajectories. The algorithm accepts as inputs

the CPS $\mathcal{M} : \mathcal{P} \times \mathbb{C}(\mathbb{R}) \times \mathbb{R} \rightarrow \mathbb{R}^n$, set of initial configuration $\subseteq \mathcal{P}$, input space given by the lower and upper bound on each input, the input discretization constant k , time-horizon T , trajectory discretization time-step Δt , and the number of trajectories N to be generated. Each trajectory is generated for a randomly selected initial configuration $x_0 \in \mathcal{I}$ (Line 8) and a randomly created input signal (lines 2 - 7). For creating k equally spaced piecewise constant input signal, the loop in line 2 iterates over k , and the inner loop (lines 3 - 5) generates a random input (u_j) using the ranges of each input. Line 6 depicts the construction of a constant input signal u_j in the time interval $[j \cdot \frac{T}{k}, (j+1) \cdot \frac{T}{k}]$. The for loop in line 9 is iterated over the trajectory discretization time points ($\lceil T/\Delta t \rceil$ many) to compute $\Gamma(j\Delta t)$. Line 11 makes a datapoint by concatenating $x_0, u, j\Delta t$, and $\Gamma(j\Delta t)$ and storing in the dataset \mathcal{D} . The input to the CPS, x_0, u , and t are the input features, and the corresponding output $\Gamma(j\Delta t) = \mathcal{M}(x_0, u, t)$ is stored as labeled output in the dataset \mathcal{D} shown in Table I. This dataset is used to learn the CPS behavior in a feed-forward deep neural network model that approximates the function $\mathcal{M}(x_0, u, t)$.

Algorithm 1 Dataset generation from CPS.

Input: The CPS $\mathcal{M} : \mathcal{P} \times \mathbb{C}(\mathbb{R}) \times \mathbb{R} \rightarrow \mathbb{R}^n$, the set of initial system configurations $\subseteq \mathcal{P}$, the input space given as a hyper-rectangle $[u_1^{lw}, u_1^{up}] \times [u_2^{lw}, u_2^{up}] \times \dots \times [u_p^{lw}, u_p^{up}]$, the input discretization k , the time-horizon $T \in \mathbb{R}$, the time-step Δt , and the number of trajectories to be generated N .

Output: The dataset \mathcal{D} stores the time discretization of N trajectories.

Initialization: $\Gamma(k) \leftarrow \emptyset, \mathcal{D} \leftarrow \emptyset$.

- 1: **for** $i = 1$ to N **do** ▷ Generate N trajectories.
- 2: **for** $j = 0$ to $k - 1$ **do** ▷ Generate a piecewise constant input signal with k equally spaced inputs.
- 3: **for** $r = 1$ to p **do** ▷ Select a random input.
- 4: $u_j[r] = \text{random}([u_r^{lw}, u_r^{up}])$
- 5: **end for**
- 6: $u([j \cdot \frac{T}{k}, (j+1) \cdot \frac{T}{k}]) = u_j$ ▷ Construct constant input signal for the intervals $[0, \frac{T}{k}], \dots, [(k-1) \cdot \frac{T}{k}, k \cdot \frac{T}{k}]$.
- 7: **end for**
- 8: Pick an initial configuration $x_0 \in \mathcal{I}$
- 9: **for** $j = 0$ to $\lceil T/\Delta t \rceil$ **do**
- 10: $\Gamma(j\Delta t) = \mathcal{M}(x_0, u, j\Delta t)$
- 11: Datapoint = $\langle x_0, [u_0, u_1, \dots, u_{k-1}], j\Delta t, \Gamma(j\Delta t) \rangle$
- 12: $\mathcal{D}.append(\text{Datapoint})$
- 13: **end for**
- 14: **end for**
- 15: **return** \mathcal{D}

TABLE I: The dataset \mathcal{D} of N trajectories. Each row is treated as labeled data for DNN construction by supervised learning.

Initial	Input signal	Time	Output
$\langle x_0^1 \rangle$	$\langle u_0^1, \dots, u_{k-1}^1 \rangle$	0	$\langle \mathcal{M}(x_0^1, u^1, 0) \rangle$
$\langle x_0^1 \rangle$	$\langle u_0^1, \dots, u_{k-1}^1 \rangle$	Δt	$\langle \mathcal{M}(x_0^1, u^1, \Delta t) \rangle$
\dots	\dots	\dots	\dots
$\langle x_0^1 \rangle$	$\langle u_0^1, \dots, u_{k-1}^1 \rangle$	$j\Delta t$	$\langle \mathcal{M}(x_0^1, u^1, j\Delta t) \rangle$
\dots	\dots	\dots	\dots
\dots	\dots	\dots	\dots
$\langle x_0^N \rangle$	$\langle u_0^N, \dots, u_{k-1}^N \rangle$	0	$\langle \mathcal{M}(x_0^N, u^N, 0) \rangle$
\dots	\dots	\dots	\dots
$\langle x_0^N \rangle$	$\langle u_0^N, \dots, u_{k-1}^N \rangle$	$j\Delta t$	$\langle \mathcal{M}(x_0^N, u^N, j\Delta t) \rangle$

2) *Data Pre-processing*: Feature scaling is a technique used in machine learning to normalize the range of input features in a dataset. It is necessary for the machine learning algorithms to interpret all the features on the same scale. If the input features

have largely varying ranges, it can lead to some features dominating the learning process, causing other features to be ignored. We apply MinMax scaling, which scales the input features in a range of 0 to 1 as follows: $\hat{x}_{l,m} = \frac{x_{l,m} - \min_m}{\max_m - \min_m}$, where $x_{l,m}$ denotes the value of feature m of record l and $\hat{x}_{l,m}$ is the corresponding normalized value. Here, \min_m and \max_m denote the minimum and maximum values of the m th input feature, respectively.

3) *Neural Network Training*: The design choice of the approximating neural network has been made following the principle of *Ockham's razor*. We learn a fully connected feed-forward neural network. For simplifying the design space exploration, the choices in the hyperparameter settings have been kept fixed, whereas the choices in the network graph structure have been explored on a trial-and-error basis.

Hyperparameter setting: The networks have been trained with *ReLU* activation function, using the Adam optimizer with a learning rate of $\lambda = 0.0001$, and on the mean squared error (MSE) loss function.

Network Graph Structure We start with a simple structure having a few hidden layers and a few nodes per layer. We gradually increase the architecture complexity by trial and error until the obtained network's performance is satisfactory. A network's performance is assessed against a fixed set of falsification instances according to our methodology using *falsification rate* as the metric.

Given a falsification instance, the *falsification rate* of a network is the number of times our framework successfully finds a counterexample out of a given number of runs using the network. A higher *falsification rate* suggests a greater likelihood of finding a counterexample using the network.

Training with Cross-Validation: We use the early-stopping algorithm that monitors the validation loss in order to stop the training before the model overfits. A *patience* value of 5 has been used. The early-stopping algorithm stops the learning iterations when the validation loss does not improve over the last *patience* many epochs. The network with the lowest validation loss over the epochs is saved. For some of the CPS (Navigation, Two-tanks, AT, and SB1), we did not use early stopping and instead trained for a fixed number of epochs, monitoring the training loss and saving the model with the lowest training loss instead. The architecture of the chosen neural network for each CPS and the hyperparameter settings used in the training process are detailed in Table II.

B. Generating a Counterexample

Once a network \mathcal{M}' is built using the dataset \mathcal{D} , the next step of our algorithm is to generate a counterexample to the given reachability specification. Our framework provides an interface to many adversarial attack algorithms and DNN verification tools which can be invoked to falsify the given reachability specification on the network \mathcal{M}' . In particular, it uses *deep neural network falsifier* (DNNF) [33], a falsification framework that reduces a reachability specification to a set of equivalent local robustness specifications. This reduction opens up the applicability of a rich class of adversarial attack algorithms such as the Fast Gradient Sign Method

(*fsgm*), Basic Iterative Method (*bim*), DeepFool, and Projected Gradient Descent (*pgd*) for falsification. In addition, our framework provides an interface to DNN verification tools via *deep neural network verifier* (DNNV) [34]. DNNV supports verification tools such as Reluplex, Neurify, and Nnenum and automatically translates the given network and property to the input format of the invoked verifier.

C. Eliminating Spurious Counterexamples

We determine whether the counterexample given by a DNN falsifier is spurious or real by simulating it in the actual CPS model. We use the simulation engine in XSPEED for CPS given as hybrid automata, and we use MATLAB for simulating CPS given as Simulink models. The simulation engine computes a trajectory from the counterexample $\mathcal{C} = (x_c, u_c, t_c)$ and checks whether the trajectory intersects with the set of unsafe configurations \mathcal{U} . If the trajectory does not intersect with \mathcal{U} , we mark the counterexample as spurious. Each spurious counterexample is stored in a set $\psi \leftarrow \psi \cup \mathcal{C}$. We remove ψ from the subsequent falsification problem by modifying the property as $(\mathcal{I}', \mathcal{U})$, where $\mathcal{I}' = \mathcal{I} - \psi$. The updated property is evaluated on the falsifier again to find a counterexample, and this process is continued until a true counterexample is found within the time and memory limit.

IV. A FALSIFICATION PROCEDURE USING DECISION-TREE

Training networks can be expensive. As an alternative, we propose a falsification procedure guided by a decision tree surrogate model of the CPS. Unlike NNFAL which is restricted to falsify reachability specification, this procedure can falsify generic Signal Temporal Logic (STL) specifications. We briefly present STL, a specification language to express the properties of CPS [27]. The syntax of an STL formula φ over a finite set of real valued variables V is defined by the following grammar:

$$\varphi ::= v \sim d \mid \neg\varphi \mid \varphi_1 \wedge \varphi_2 \mid \varphi_1 U_I \varphi_2$$

where $v \in V$, $\sim \in \{<, \leq\}$, $d \in \mathbb{Q}$ is a Rational, and $I \subseteq \mathbb{R}^+$ is an interval. The semantics of STL is given with respect to a *signal*, which in the context of CPS is a trajectory Γ . Γ_v denotes the projection of Γ on $v \in V$.

Definition 4 (STL Semantics [27]): We denote $(\Gamma, t) \models \varphi$ to mean that a finite trajectory $\Gamma : [0, T] \rightarrow \mathbb{R}^n$ satisfies the STL property φ at the time point $t \in [0, T]$. The rules of satisfaction are as follows:

$$\begin{aligned} (\Gamma, t) \models v \sim d &\Leftrightarrow \Gamma_v(t) \sim d & (1) \\ (\Gamma, t) \models \neg\varphi &\Leftrightarrow (\Gamma, t) \not\models \varphi & (2) \\ (\Gamma, t) \models \varphi_1 \wedge \varphi_2 &\Leftrightarrow (\Gamma, t) \models \varphi_1 \text{ and } (\Gamma, t) \models \varphi_2 & (3) \\ (\Gamma, t) \models \varphi_1 U_I \varphi_2 &\Leftrightarrow \exists t' \in (t + I) \cap T : (\Gamma, t') \models \varphi_2 \\ &\text{and } \forall t'' \in (t, t'), (\Gamma, t'') \models \varphi_1 & (4) \end{aligned}$$

The temporal operators *always* (\square_I) and *eventually* (\diamond_I) are defined using the *until* operator as:

$$\square_I \varphi = \neg(\top U_I \neg\varphi), \quad \diamond_I \varphi = \top U_I \varphi.$$

TABLE II: The table shows the details of neural networks learned from the CPS trajectories. *#Network Layers* is the number of hidden layers in the neural network. *Architecture* shows the number of neurons in each hidden layer. Hyperparameters show the epochs and the batch size. *Dataset Size* shows the number of data entries (in Millions) in the dataset. *Learning Time* shows the time taken to train the network. *Dataset Generation Time* is the time to produce the dataset from the CPS.

CPS	#Network Layers	Architecture	Hyperparameters		Dataset Size (Millions)	Learning Time (Hours)	Dataset Generation Time (Secs)
			Epochs	Batch-Size			
Oscillator	6	$512 \times 256 \times 128 \times 64 \times 32 \times 16$	16	256	6.1	0.3	79
Two tanks	5	$512 \times 256 \times 128 \times 64 \times 32$	200	256	8.2	4.3	71
Navigation	6	$512 \times 256 \times 128 \times 64 \times 32 \times 16$	200	256	11.8	3.6	318
Bouncing ball	7	$512 \times 256 \times 256 \times 128 \times 128 \times 64 \times 32$	21	256	7.2	0.7	36
ACC	5	$512 \times 256 \times 128 \times 64 \times 32$	19	256	6.5	0.5	98
AGCAS	5	$512 \times 256 \times 128 \times 64 \times 32$	54	128	3.5	1.4	1622
CC	5	$512 \times 256 \times 128 \times 64 \times 32$	7	256	33.3	0.7	743
AT	5	$512 \times 256 \times 128 \times 64 \times 32$	150	256	10	4	1251
AFC	5	$512 \times 256 \times 128 \times 64 \times 32$	30	256	33.6	2.3	3022
SBI	5	$512 \times 256 \times 128 \times 64 \times 32$	200	16	0.05	0.1	151.74

Informally, $\Box_{(a,b)}\varphi$ is true if φ holds at all times within the interval (a, b) , whereas $\Diamond_{(a,b)}\varphi$ is true if φ holds at some time within (a, b) .

A. Robustness of a Trajectory

The notion of *robustness* [10] of a trajectory to a given STL specification evaluates how "closely" the trajectory satisfies a specification. Mathematically, it is a real-valued function $\rho(\varphi; \Gamma, t) \in \mathbb{R}$, which measures the degree of satisfaction of φ by Γ at time point t . The notion of satisfaction of a specification is lifted from a yes/no answer to a quantitative measure. We utilize the notion of robustness of CPS trajectories to classify them using a decision tree based on their "closeness" to violating a given STL safety specification. A formal description of robustness is given as follows.

$$(\Gamma, t) \models \varphi \iff \rho(\varphi; \Gamma, t) \geq 0,$$

$$(\Gamma, t) \not\models \varphi \iff \rho(\varphi; \Gamma, t) < 0.$$

For atomic predicates $v \sim d$, the robustness is defined as:

$$\rho(v \sim d; \Gamma, t) = d - \Gamma_v(t).$$

The robustness of complex STL formulas is defined as:

$$\rho(\neg\varphi; \Gamma, t) = -\rho(\varphi; \Gamma, t), \quad (5)$$

$$\rho(\varphi_1 \wedge \varphi_2; \Gamma, t) = \min(\rho(\varphi_1; \Gamma, t), \rho(\varphi_2; \Gamma, t)), \quad (6)$$

$$\rho(\varphi_1 U_I \varphi_2; \Gamma, t) = \max_{t' \in (t+I) \cap [0, T]} (\min(\rho(\varphi_2; \Gamma, t'), \inf_{t'' \in [t, t']} \rho(\varphi_1; \Gamma, t''))). \quad (7)$$

The robustness of derived operators are defined as follows:

$$\rho(\Diamond_I \varphi; \Gamma, t) = \max_{t' \in (t+I) \cap [0, T]} \rho(\varphi; \Gamma, t'),$$

$$\rho(\Box_I \varphi; \Gamma, t) = \min_{t' \in (t+I) \cap [0, T]} \rho(\varphi; \Gamma, t').$$

We mention $\rho(\varphi; \Gamma)$ to mention the robustness of the trajectory at time $t = 0$, that is $\rho(\varphi; \Gamma, 0)$. We now state the CPS falsification problem addressed in this section.

Problem Statement 2: Given a CPS $\mathcal{M} : \mathcal{P} \times \mathbb{C}(\mathbb{R}) \times \mathbb{R} \rightarrow \mathbb{R}^n$, an initial set of configurations $\mathcal{I} \subseteq \mathcal{P} \times \mathbb{C}(\mathbb{R}) \times \mathbb{R}$ and a STL safety specification φ , find a tuple $\mathcal{C} = (x_c, u_c, t_c)$, an

element of \mathcal{I} such that the trajectory $\Gamma : [0, t_c] \rightarrow \mathbb{R}^n$ of \mathcal{M} starting from an initial configuration x_c , with an input signal u_c over a time horizon t_c has robustness $\rho(\varphi; \Gamma) < 0$.

The first step is to construct the dataset using a CPS simulator in a similar way we generated the dataset for building a DNN, but now using the robustness of CPS trajectories as the output feature. A decision tree (\mathcal{M}') is learned from the generated data set. The decision tree is then traversed to find the leaf nodes that classify trajectories violating the given safety specification, that is with robustness less than 0. If there is no such leaf node, then our algorithm finds the leaf node that characterizes the trajectories *closest* to violating the safety specification. An explanation for violating the safety specification is then extracted by backtracking the path from the identified *leaf* node to the root and conjoining the respective branching conditions. This is the learned insight that a decision tree provides on the input-space, by telling us that trajectories initiating from this space is likely to violate the specification. Consequently, using the explanation condition, a specified number of random simulations are computed. The last step of the algorithm is to check whether the simulations provide us with the required number of counterexamples. If so, the algorithm terminates by outputting the counterexamples. Otherwise, we append the dataset with the generated simulation traces and retrain and refine the decision tree model again. The steps of generating explanations and computing random simulations are repeated. The proposed algorithm terminates when the desired number of counterexamples are obtained, or when the execution budget is exceeded. We consider the execution budget as the number of retraining iterations permitted for the algorithm. Algorithm 3 describes the falsification procedure, referred to as Decision Tree-based Falsification (DTFAL). The left part of Figure 1 illustrates the DTFAL procedure, the details of which are discussed in the subsequent sections.

B. CPS to Decision-Tree

1) *Dataset Generation:* Unlike the earlier dataset, which focused on capturing the system's general input-output behavior, this dataset enables us to classify the trajectories based on their robustness measure. This specialization enhances the decision tree's ability to identify regions of the input space where the system is likely to violate the safety specification.

The dataset is generated from the CPS using the simulators discussed in Section III-A1 together with an STL monitoring tool Breach [9], which evaluates the robustness of the trajectory with respect to a specified STL safety specification. The input features of the dataset are the components of the initial configuration of the CPS \mathcal{I} , that is an initial state $\langle x_i \rangle$, and a piecewise constant input signal $\langle u^i \rangle \in \mathbb{C}(\mathbb{R})$, represented as a vector, element of $\mathbb{R}^{k \times m}$. All trajectories are computed over the same time-horizon and therefore, time-horizon is not captured in the dataset. The output feature is a robustness measure of the trajectory, computed with respect to the given STL safety specification. The structure of the dataset for building a decision tree is shown in Table III.

TABLE III: The dataset \mathcal{D} of N trajectories for an STL safety specification φ . Each row is treated as labeled data for Decision-Tree construction. $\rho(\varphi; \Gamma^i)$ is the robustness value of the i -th trajectory.

Initial state	Input signal	Output
$\langle x_0^1 \rangle$	$\langle u_0^1, \dots, u_{k-1}^1 \rangle$	$\rho(\varphi; \Gamma^1)$
$\langle x_0^2 \rangle$	$\langle u_0^2, \dots, u_{k-1}^2 \rangle$	$\rho(\varphi; \Gamma^2)$
$\langle x_0^3 \rangle$	$\langle u_0^3, \dots, u_{k-1}^3 \rangle$	$\rho(\varphi; \Gamma^3)$
\dots	\dots	\dots
$\langle x_0^N \rangle$	$\langle u_0^N, \dots, u_{k-1}^N \rangle$	$\rho(\varphi; \Gamma^N)$

2) *Decision-Tree Building*: We used *sklearn* (Scikit-learn), a data modeling library in Python to build the Decision Tree. Specifically, the *DecisionTreeRegressor* method has been used. The method uses the CART [6] algorithm that builds a binary tree in which leaf nodes represent the predicted output features and intermediate nodes, also known as decision nodes, are where decision choices are made. We used the default parameter settings in *DecisionTreeRegressor*.

When the algorithm meets a stopping criterion in a node, the node is designated as a leaf node. The value of a leaf node is the mean of the datapoint of the target attribute in that node, in our case, which is the robustness value of the trajectories.

C. Generating Explanations to Safety Property Violation

1) *Finding Falsifying Leaf Nodes*: Once we approximate the actual CPS with the Decision Tree \mathcal{M}' from the dataset \mathcal{D} , our algorithm generates an explanation for the violation of a given STL safety specification by \mathcal{M}' . The initial phase for generating the explanation is the retrieval of all leaf nodes from the decision tree \mathcal{M}' , followed by filtering the leaf nodes that characterize trajectories that are likely to violate the safety specification. Every leaf node is associated with a predicted robustness measure of the trajectories that map to that node. If a leaf node's robustness measure is less than 0, it classifies the trajectories that are safety violating. We designate such a node as *falsifying leaf node*.

Definition 5 (Falsifying leaf node): A falsifying leaf node of the decision tree \mathcal{M}' is defined as a leaf node \mathcal{L} such that $\mathcal{L}_\rho < 0$, where \mathcal{L}_ρ is the node's predicted robustness measure. Consider a decision tree in Figure 2a for an illustration. The only *falsifying leaf node* in this example is highlighted in

Red. If no falsifying leaf node is found in the decision tree, our algorithm finds the *nearest falsifying leaf node(s)*, that is, nodes with robustness value closest to 0. The *nearest falsifying leaf nodes* are then referred to generate an explanation. The definition of *nearest falsifying leaf node* is as follows:

Definition 6 (Nearest falsifying leaf node): Given a decision tree \mathcal{M}' and given that \mathcal{M}' has no falsifying leaf node, we define a nearest falsifying leaf node \mathcal{L}_{near} to be a leaf node with predicted robustness value closest to zero.

$$\mathcal{L}_{near} = \arg \min_{l \in leaf} l_\rho$$

where l_ρ is the predicted robustness value of leaf l , and l_ρ is its predicted robustness measure.

The illustrative decision tree in Figure 2b shows the nearest falsifying leaf node in Red. Algorithm 2 describes the procedure for finding the nearest falsifying leaf nodes.

Algorithm 2 FIND_NEAREST_LEAF_NODE(\mathcal{M}')

Input: A Decision Tree \mathcal{M}' .

Output: A set of falsifying leaf nodes \mathcal{L}_{near} .

Initialization: $\mathcal{L}_{near} \leftarrow \emptyset$; $m = \infty$ \triangleright Initialize min robustness to infinity.
 $leaf \leftarrow \text{FIND_ALL_LEAFS}(\mathcal{M}')$
for $l \in leaf$ **do**
 if $|l_\rho| < m$ **then**
 $m = |l_\rho|$ \triangleright Update minimum robustness value.
 end if
end for
for $l \in leaf$ **do**
 if $|l_\rho| = m$ **then**
 $\mathcal{L}_{near} \leftarrow \mathcal{L}_{near} \cup \{l\}$ \triangleright Add leaf nodes with robustness value m .
 end if
end for
return \mathcal{L}_{near}

2) *Generating Explanations*: Once a *falsifying leaf node* is identified, our algorithm generates an explanation to violating a safety specification. To place the definition of explanation, we present a few notations. The input features of a decision tree are represented by the set $X = \{x_1, x_2, \dots, x_n\}$ of n real-valued variables. A valuation v is an assignment of a real value to each variable $x \in X$. We now define an explanation, the central idea to the falsification algorithm.

Definition 7 (explanation): Given a decision tree \mathcal{M}' with a set \mathcal{X} of n input features and an STL safety specification φ , an explanation for violating φ by \mathcal{M}' is defined as a predicate $Exp_{\mathcal{M}'}(\mathcal{X})$ over the free variables in \mathcal{X} such that there exists a valuation v of \mathcal{X} , where $Exp_{\mathcal{M}'}(v)$ is true and $\mathcal{M}'(v) < 0$. The set of all valuations that satisfy the explanation predicate describes a region of inputs $\subseteq \mathcal{I}$ to the decision tree which contains a counterexample to the safety specification. Our algorithm constructs an explanation by traversing the decision tree from the *falsifying leaf node* to the root, conjoining the decision-making condition at each intermediate node, to form a predicate that is a conjunction of linear constraints. The process of collecting the decision-making conditions along the path from *falsifying leaf node* to the root is discussed in Algorithm 4. Initially, the explanation predicate is set to *true*. While traversing upward in the tree from a leaf node, if the current node is *left child*, the decision-making condition of its parent node is conjoined with the explanation predicate. On the other hand, if the current node is a *right child*, the

the CART algorithm. Line 4 finds the falsifying leaf nodes (\mathcal{L}). Line 6 states that if \mathcal{M}' has no falsifying leaf node, then our algorithm finds the nearest falsifying leaf nodes. The for loop in lines 8 - 16 iterates over the leaf nodes \mathcal{L} , identifying the explanation ($Exp_{\mathcal{M}'}$) to the violation of φ and subsequently determining the true counterexamples. Line 9 finds the explanation ($Exp_{\mathcal{M}'}$) using the procedure defined in Algorithm 4. In the procedure SIMULATOR in line 10, R many valuations are randomly selected that satisfy the explanation $Exp_{\mathcal{M}'}$. From these R valuations, R random trajectories are simulated, and their robustness is observed to see how many qualify to be counterexamples. This function also generates the dataset ($traj_data$) from the R trajectories, which is used to retrain the decision tree, if required. If the number of counterexamples (CE) reaches the required minimum threshold within the execution budget, the algorithm terminates and displays the CE counterexamples. Otherwise, failure is returned.

V. RESULTS

Benchmarks The framework has been evaluated on falsification problem instances from 9 CPS out of which 6 have linear dynamics (Navigation [13], Oscillator [14], Two tanks [17], Bouncing ball, Adaptive Cruise Controller (ACC) [7], and Chasing Cars (CC) [19]) and three have non-linear dynamics (Aircraft Ground Collision Avoidance System (F16) [16], Automatic Transmission (AT) [18], and Fuel Control of an Automotive Powertrain (AFC) [20]). Recently, a procedure for creating synthetic benchmarks has been recently introduced in [39] for testing the strength of falsification methods. We considered five Synthetic Benchmarks (SB) from that paper, each involving an LSTM model trained on a synthetic dataset designed for a specific safety property. We now briefly describe the models and the specifications, some of which are from the annual friendly tool competition ARCH-COMP 2024 [22], in the falsification category. The safety specifications in signal temporal logic (STL) are shown in Table IV.

A. Implementation and Experimental Setup

The framework is implemented in a tool FLEXIFAL and offers the two falsification strategies to a user, namely NNFAL and DTFAL. The tool provides a command-line interface. The source code of FLEXIFAL, the command-line options and user instructions are made publicly available on GitLab [https://gitlab.com/Atanukundu/FlexiFal]. We evaluate FLEXIFAL on Ubuntu 22.04.5, 64 GB RAM with 6 GB GPU, and a 5 GHz 12-core Intel i7-12700K processor. For the evaluation of NNFAL, we build the neural network surrogates of CPS in advance. The neural networks were trained in Google Colab, with Intel Xeon 2.20 GHz CPU, 12.7 GB RAM with 15 GB Tesla T4 GPU, and Ubuntu 20.04. In order to quantify the difficulty level of a falsification instance, specifically for the hybrid automata instances, we define a degree of difficulty (DoD) metric, which is the percentage of the falsifying trajectories in N randomly simulated trajectories. The lower the DoD, the harder it is to falsify the instance. All experiments have 1 hour timeout and a maximum memory usage limit of 6

GB. We test each falsification instance ten times and report the success rate and the average falsification time of the successful tests. In the following performance comparison table, the gray cells highlight the algorithms or tools that demonstrate the best time to falsify the respective instances. The results of the experiments provide a response to the following research questions.

RQ1: Which out of DTFAL and NNFAL is more effective in falsifying CPS instances?

RQ2: How does FLEXIFAL compare with state-of-the-art CPS falsification tools?

RQ3: Can FLEXIFAL find multiple counterexamples efficiently?

B. RQ1: NNFAL vs DTFAL

Table V demonstrates the empirical results of executing NNFAL and DTFAL on several falsification instances. We describe the choice of parameters and a performance comparison.

a) *Evaluation using NNFAL* : Recall that NNFAL provides a repertoire of neural network adversarial attack algorithms and network verification tools via the DNNF and DNNV interface. We report the performance of NNFAL using adversarial attack algorithms as well as using neural network verification tools supporting falsification. The falsification instances are evaluated using four attack algorithms, namely *pgd* [26], *fgsm* [15], *bim* [25], and *ddnattack* [31]. In the table for NNFAL, we show the result of the fastest algorithm to falsify. The fastest in our experiments turns out to be *pgd*. Furthermore, all falsification instances are also evaluated using three neural network verification tools, namely *Reluplex* [21], *Neurify* [38], and *Nnenum* [5]. We observe that *Nnenum* is the fastest to falsify in our experiments, and thus we report results on *Nnenum* for NNFAL. Our findings indicate that falsification with NNFAL generates novel counterexamples that are unseen in the dataset. The results show that *Nnenum* finds counterexamples faster compared to *pgd* in most instances. However, for hard instances (very low DoD), *Nnenum* fails in the falsification task, where *pgd* is successful in a reasonable time. The observations, therefore, do not conclude that verification tools of deep neural networks are more effective than local robustness property falsifiers or vice versa for CPS falsification. Rather, we conclude that they have complementary strengths, and we can therefore reap the benefits of these techniques with our framework. Note that the time to build the neural network is not included in the falsification time for NNFAL. We choose to do so because the falsification algorithms need not construct the network every time a new specification is given for falsification. The networks, once constructed, can be reused for falsification tasks. Since NNFAL is limited to falsification of reachability specifications, it could not falsify many of the instances in our set which had generic STL properties. Such instances are marked with NA against NNFAL in the table. Overall, it could falsify 14 out of 37 instances.

b) *Evaluation using DTFAL*: The reported falsification time includes the time to train the decision tree since decision tree learning is specification dependent. The algorithm is

TABLE IV: Safety specifications are given in STL. Dims is the sum of the number of system variables and input variables in the CPS. DoD is the percentage of safety-violating trajectories of 2000 simulated trajectories.

Instance	CPS	Dims	DoD	Safety Specification in Signal Temporal Logic
TT1	Two tanks	3	0.32%	$\Box_{[0,10]} \neg ((x1 \geq 0) \wedge (x1 \leq 0.40) \wedge (x2 \geq -0.500) \wedge (x2 \leq -0.465))$
TT2		3	0.83%	$\Box_{[0,10]} \neg ((x1 \geq -0.20) \wedge (x1 \leq 0.20) \wedge (x2 \geq 0.31) \wedge (x2 \leq 0.35))$
TT3		3	2.68%	$\Box_{[0,10]} \neg ((x1 \geq -0.20) \wedge (x1 \leq 0.20) \wedge (x2 \geq 0.30) \wedge (x2 \leq 0.35))$
TT4		3	2.95%	$\Box_{[0,10]} \neg ((x1 \geq 1) \wedge (x1 \leq 1.5) \wedge (x2 \geq -0.4) \wedge (x2 \leq -0.23))$
NAV1	Navigation	3	0.003%	$\Box_{[0,50]} \neg ((x1 \geq 7) \wedge (x1 \leq 8) \wedge (x2 \geq 9) \wedge (x2 \leq 10))$
NAV2		3	0.07%	$\Box_{[0,50]} \neg ((x1 \geq 22) \wedge (x1 \leq 23) \wedge (x2 \geq 11) \wedge (x2 \leq 12))$
NAV3		3	2.77%	$\Box_{[0,50]} \neg ((x1 \geq 11) \wedge (x1 \leq 12) \wedge (x2 \geq 16) \wedge (x2 \leq 17))$
OSC1	Oscillator	3	0.15%	$\Box_{[0,10]} \neg ((p \geq 0) \wedge (p \leq 0.1) \wedge (q \geq 0.13485) \wedge (q \leq 0.15))$
OSC2		3	0.29%	$\Box_{[0,10]} \neg ((p \geq -0.50) \wedge (p \leq -0.45029) \wedge (q \geq 0.1) \wedge (q \leq 0.1968))$
OSC3		3	0.41%	$\Box_{[0,10]} \neg ((p \geq 0.100) \wedge (p \leq 0.193) \wedge (q \geq -0.30) \wedge (q \leq -0.25))$
BB1	Bouncing ball	3	1.2%	$\Box_{[0,10]} \neg ((v \geq -1) \wedge (v \leq 1) \wedge (x \geq 1) \wedge (x \leq 2))$
ACC1	ACC	10	0%	$\bigwedge_{i=0..3} \Box_{[0,10]} (x_i > x_{i+1})$
F16	F16	16	0.1%	$\Box_{[0,15]} (altitude > 0)$
CC1	CC	7	0.60%	$\Box_{[0,100]} (y_5 - y_4 \leq 40)$
CC2		7	0%	$\Box_{[0,70]} \Diamond_{[0,30]} y_5 - y_4 \geq 15$
CC3		7	1.15%	$\Box_{[0,80]} ((\Box_{[0,20]} y_2 - y_1 \leq 20) \vee (\Diamond_{[0,20]} y_5 - y_4 \geq 40))$
CC4		7	0%	$\Box_{[0,65]} \Diamond_{[0,30]} \Box_{[0,5]} y_5 - y_4 \geq 8$
CC5		7	1.45%	$\Box_{[0,72]} \Diamond_{[0,8]} ((\Box_{[0,5]} y_2 - y_1 \geq 9) \rightarrow (\Box_{[5,20]} y_5 - y_4 \geq 9))$
CCx		7	0.55%	$\bigwedge_{i=1..4} \Box_{[0,50]} (y_{i+1} - y_i > 7.5)$
AT1	AT	5	0%	$\Box_{[0,20]} (v < 120)$
AT2		5	4.55%	$\Box_{[0,10]} (\omega < 4750)$
AT51		5	9.05%	$\Box_{[0,30]} ((\neg g1 \wedge \circ g1) \rightarrow \circ \Box_{[0,2.5]} g1),$ where $\circ \phi \equiv \Diamond_{[0.001,0.1]} \phi$
AT52		5	5.55%	$\Box_{[0,30]} ((\neg g2 \wedge \circ g2) \rightarrow \circ \Box_{[0,2.5]} g2)$
AT53		5	6.05%	$\Box_{[0,30]} ((\neg g3 \wedge \circ g3) \rightarrow \circ \Box_{[0,2.5]} g3)$
AT54		5	3.1%	$\Box_{[0,30]} ((\neg g4 \wedge \circ g4) \rightarrow \circ \Box_{[0,2.5]} g4)$
AT6a		5	0.25%	$(\Box_{[0,30]} \omega < 3000) \rightarrow (\Box_{[0,4]} v < 35)$
AT6b		5	0.1%	$(\Box_{[0,30]} \omega < 3000) \rightarrow (\Box_{[0,8]} v < 50)$
AT6c		5	0.15%	$(\Box_{[0,30]} \omega < 3000) \rightarrow (\Box_{[0,20]} v < 65)$
AT6abc		5	0.35%	$AT6a \wedge AT6b \wedge AT6c$
AFC27	AFC	4	1.5%	$\Box_{[11,50]} ((rise \vee fall) \rightarrow (\Box_{[1,5]} \mu < 0.008))$ where $rise = (\theta < 8.8 \wedge \Diamond_{[0,0.05]} \theta > 40.0)$ $fall = (\theta > 40.0 \wedge \Diamond_{[0,0.05]} \theta < 8.8)$
AFC29		4	7.95%	$\Box_{[11,50]} (\mu < 0.007)$
AFC33		4	8.2%	$\Box_{[11,50]} (\mu < 0.007)$
SB1	SB-1	3	0%	$\Box_{[0,24]} (b < 20)$
SB2	SB-2	2	0%	$\Box_{[0,18]} (b > 90 \vee \Diamond_{[0,6]} b < 50)$
SB3	SB-3	3	0.05%	$(\Diamond_{[6,12]} b > 10) \rightarrow (\Box_{[18,24]} b > -10)$
SB4	SB-4	4	0%	$\Box_{[0,19]} ((\Box_{[0,5]} b_1 \leq 20) \vee (\Diamond_{[0,5]} b_2 \geq 40))$
SB5	SB-5	3	0%	$\Box_{[0,17]} (\Diamond_{[0,2]} \neg ((\Box_{[0,1]} b_1 \geq 9) \vee (\Box_{[1,5]} b_2 \geq 9)))$

invoked with a command to generate one counterexample and allowing maximum 1 retraining. The size of the dataset and the number of random simulations to search from an explanation are chosen on a trail and error basis, with the goal of keeping it as small as possible and at the same time succeeding in falsification. We observe that DTFAL shows high falsification rate in most of the instances and more importantly, it displays high success rate, falsifying 33 out of 37 instances. The falsification time in DTFAL is better than NNFAL in most instances. Overall, we can conclude that DTFAL is more effective than NNFAL in our experiments. Figure 3 depicts counterexamples generated by NNFAL on Oscillator, Navigation, and ACC. Figure 4 and 5 show the counterexamples obtained by DTFAL on some of the benchmark instances.

C. RQ2 Comparison with CPS falsification tools

We present a comparison of FLEXIFAL with the falsification tools that participated in ARCH-COMP 24 [22]. The performance of these tools is shown in Table VI. The data shown in the table is from the ARCH-COMP 2024 [22] report, except the appended results of FLEXIFAL. Participating tools

use different methodologies, making it challenging to decide on the comparison metrics and judging the best-performing tool. Over the past editions of the competition, falsification rate (FR) along with the mean number of simulations (\bar{S}) required to falsify an instance are the agreed upon metrics that each participating tool report. The primary objective of the competition is to report the state-of-the-art falsification tools, highlighting their strengths and limitations for different benchmarks. We observe that FREAK requires a very small number of simulations to falsify the instances among the other tools. However, it cannot falsify F16 and AFC33, where DTFAL succeeds. The falsification rate (FR) is nearly the same for all the instances among the tools. The mean number of simulations needed to falsify an instance varies considerably across the tools. We see that DTFAL algorithm of FLEXIFAL finds counterexamples in most of the instances with high FR rate. However, it generally requires a larger number of simulations than the others. On the brighter side, DTFAL identifies counterexamples in instances such as F16 and AFC33, which most of the other tools fail to falsify. We therefore believe that FLEXIFAL is competent among the state-of-the-art.

TABLE V: FR stands for falsification rate, the number of successful runs out of 10 for which our framework finds a counterexample (CE). In DTFAL, DG denotes the time taken to generate the training dataset, while Train represents the time to train the decision tree, including the retrainings if necessary. Search refers to the time to find counterexamples using the generated explanations. Fal represents the total time to identify a counterexample, calculated as the sum of DG, Train, and Search time. In NNFAL, TT is the neural network training time. MR shows the maximum number of search refinements to eliminate spurious CEs before finding a valid one. Avg time is the average time that *pgd* takes to find a valid CE, calculated over successful runs. Val is the average time taken by NNFAL to validate the CE on the actual CPS across the successful runs, incorporating the time required for spurious ce checking and the specification modifications before the true CE is encountered. Fal Time in an adversarial attack algorithm is the sum of Avg and Val over the successful runs. Fal Time in the DNN verification tool is similarly the sum of falsification time and validation time for the respective instances. Times are reported in seconds except in the TT column, which shows time in hours. NA indicates that the respective algorithm does not support the instance.

Instance	DTFAL					NNFAL											
	FR	Time				TT	Adversarial Attack Algorithm (<i>pgd</i>)					DNN Verification Tool (<i>nenum</i>)					
		DG	Train	Search	Fal		FR	MR	Avg Time	Val	Fal Time	FR	MR	Time	Val	Fal Time	
TT1	10	6.6	0.35	0.17	7.12	4.3	10	1	150.80	0.32	151.12	10	0	1.78	0.26	2.04	
TT2	10	1.64	0.03	0.18	1.85		10	0	996.66	0.25	996.91	10	0	4.00	0.26	4.26	
TT3	10	1.67	0.03	0.17	1.87		10	0	62.94	0.25	63.19	10	0	3.33	0.27	3.60	
TT4	10	1.61	0.03	0.17	1.81		10	0	23.41	0.28	23.69	10	0	1.51	0.27	1.78	
Osc1	10	6.99	0.37	0.26	7.62	0.3	10	0	0.24	0.28	0.52	10	0	1.60	0.31	1.91	
Osc2	10	7.11	0.35	0.20	7.66		10	5	70.04	1.68	71.72	6	9	22.47	1.85	Timeout	
Osc3	10	1.09	0.005	0.19	1.28		10	5	1091.07	5.25	1096.32					Timeout	
NAV1	10	133.33	12.95	1.83	148.11	3.6	7	2	14.16	3.11	17.27					Timeout	
NAV2	10	14	0.75	1.80	16.55		10	0	3.20	1.38	4.58	10	3	3.65	2.68	6.33	
NAV3	10	2.88	0.04	0.86	3.78		0				Timeout					Error	
BB1	10	1.61	0.73	0.17	2.51	0.5	10	3	0.09	0.40	0.49	10	1	1.40	0.37	1.77	
ACC1	10	1.24	0.007	0.22	1.47	1.4	10	0	0.11	23.54	23.65	10	0	2.21	23.36	25.57	
F16	10	469.52	0.176	67.40	537.09						Timeout					OOM	
CC1	10	72.33	15.48	7.53	95.34	0.7					NA					NA	
CC2	10	97.96	11.41	17.96	127.33						NA						NA
CC3	10	72.88	8.88	1.27	83.03						NA						NA
CC4					Timeout						NA						NA
CC5	10	75.47	3.90	4.11	83.48						NA						NA
CCx	10	147.72	8.98	56.34	213.04	10	0	0.15	46.35	46.50	5	0	1.70	40.70	42.40		
AT1					Timeout	1	2	0.10	72.44	72.54	1	4	96.79	46.45	143.24		
AT2	10	13.95	0.30	1.90	16.15	4.0					OOM					Error	
AT51	10	17.74	0.22	1.15	19.11						NA						NA
AT52	10	14.19	0.17	2.34	16.70						NA						NA
AT53	10	14.34	0.22	2.34	16.90						NA						NA
AT54	10	14.19	0.14	2.04	16.37						NA						NA
AT6a	10	42.52	2.25	0.38	45.15						OOM						Timeout
AT6b	10	65.68	3.35	3.45	72.48						OOM						Timeout
AT6c	10	43.19	1.34	8.20	52.73		2	1	0.01	46.23	46.24						Timeout
AT6abc	10	43.76	1.31	1.49	46.56						OOM						OOM
AFC27	10	26.85	1.33	4.84	33.02		2.3					NA					NA
AFC29	10	26.95	0.88	1.89	29.72						Timeout						Timeout
AFC33	10	25.28	0.67	1.86	25.28						Timeout						Timeout
SB1	5	3182.71	10.43	17.67	3210.81	0.1					OOM					Timeout	
SB2					Timeout						NA					NA	
SB3	10	52.72	0.02	11.92	64.66						NA					NA	
SB4	10	1951.45	3.14	88.97	2043.56						NA					NA	
SB5					Timeout						NA					NA	

TABLE VI: A Comparison with the CPS falsification tools. FR is the falsification rate. \bar{S} is the mean number of simulations needed to falsify the respective instances. The blank in the table indicates that the respective tools could not falsify the instances.

Tool Approach	UR		ARISTEO ARX-2		ATheNA		EXAM-Net		FalCAun		ForeSee		FReak		Moonlight		FlexiFal (DTFal)		OD		$\Psi - TaLiRo$ ConBo-LS		$\Psi - TaLiRo$ PART-X		
	FR	\bar{S}	FR	\bar{S}	FR	\bar{S}	FR	\bar{S}	FR	\bar{S}	FR	\bar{S}	FR	\bar{S}	FR	\bar{S}	FR	\bar{S}	FR	\bar{S}	FR	\bar{S}	FR	\bar{S}	
Instance F16															10	21	10	371.72							
CC1	10	16.4	10	11.3	10	60.5	10	36.1	10	396	10	21.8	10	3			10	169.90	10	61.2	10	18	10	17.6	
CC2	10	12.4	10	10.5	10	94	9	398.6	10	76	8	224.3	10	3			10	241.09	4	109.3	10	14.8	10	17.8	
CC3	10	19.6	10	18.8	10	119.2	10	14.9	10	122	10	36.1	10	2.6			10	152.1	10	35.2	10	11.4	10	13.5	
CC4					2	514			4	1256	7	680	10	1349.9							1	1387			
CC5	10	37.4	10	29.1	9	112	10	78.2			10	88.7	10	47.5			10	523.1	10	55.7	10	32.3	10	29.9	
CCx	6	396.7	9	610.4	5	86.4	10	448.1			10	228	7	1723.6			10	468.66	2	261.5	10	244.2	10	607	
AT1							10	150.4	10	896	10	387.4	10	4.5			10			5	1131.7	10	30.5		
AT2	10	18.8	10	15.1	10	62.3	10	22.7	10	256	9	196.6	10	2.2			10	51	10	18.5	10	13.7	10	6.5	
AT51	10	20.5	1	1371	10	106	10	8.5			10	15	10	17.7			10	57.78	10	11.6	10	10.1	10	13.3	
AT52	10	74.1	10	4.4	10	19	10	10.3			10	65.7	10	5.2			10	52.8	10	8.6	10	67.8	10	66.5	
AT53	10	1.5	10	4.4	10	2.2	10	1.5			10	4.3	10	3.9			10	53.1	10	2.2	10	4.1	10	2.2	
AT54	10	47.9	6	571.5	10	138.9	10	89.6			10	60.3	10	103			10		10	18.4	10	37.4	10	85	
AT6a	10	156.6	8	271.4	10	245.5	10	61.1	10	1002	10	115.2	10	24.6			10	197.9	10	64.3	10	304.5	10	153.7	
AT6b	10	472.2	6	536	9	279.3	10	119.4			10	253.9	10	17.4			10	314.2	10	122	6	782.2	10	307.9	
AT6c	10	326.8	8	643.8	10	194.5	10	176.5	10	898	10	133.1	10	15.5			10	292.2	10	118.5	9	472.1	10	334.4	
AT6abc	10	149	8	505.2	10	234.4	10	57.4	10	1232	10	123.6	10	13.1			10	220.8	10	61.3	10	139.2	10	106.9	
AFC27			9	56.2	8	137.8	10	235.8					10	12			10	25.7	10	391.2	10	101.8	10	34.3	
AFC29	10	25.1	10	3.9	10	18.6	10	8.5					10	3.1			10	21	10	13	10	9.1	10	12.1	
AFC33																	10	21							

Fig. 3: Counterexamples generated by FLEXIFAL using NNFAL algorithm.

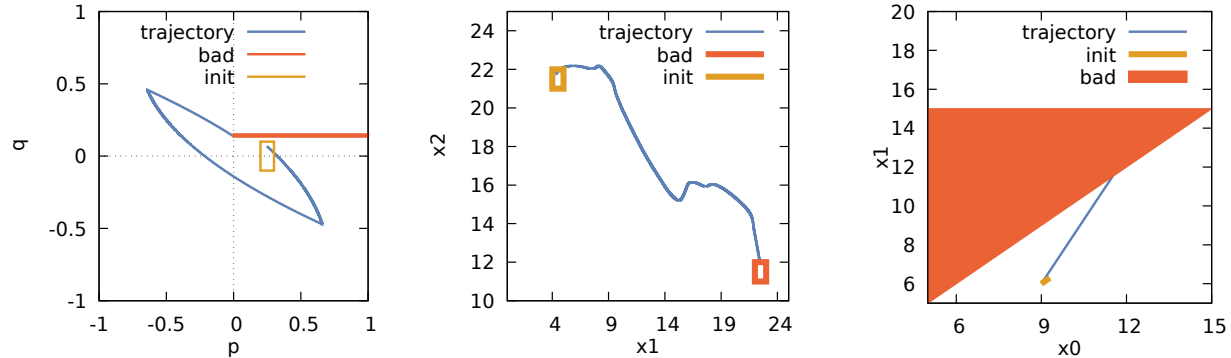


Fig. 4: Counterexamples generated by FLEXIFAL using DTFAL algorithm.

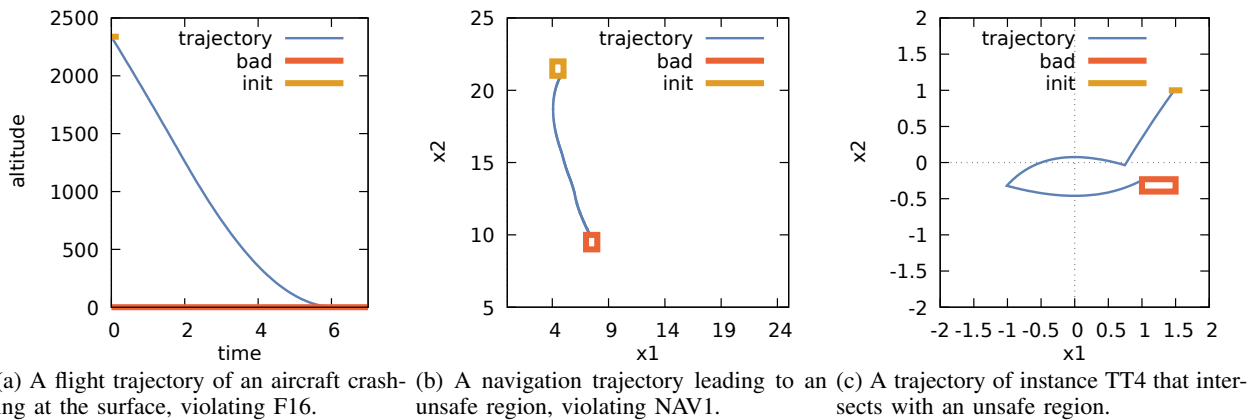
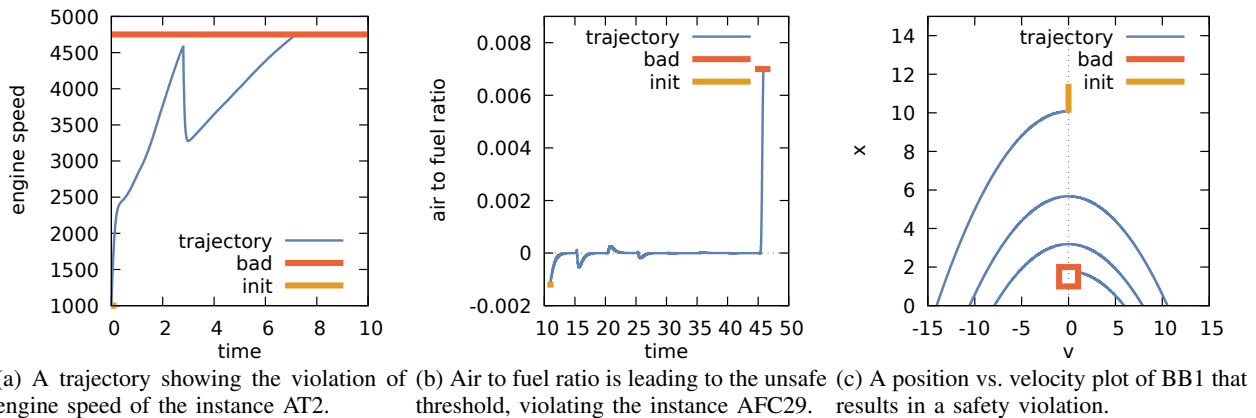


Fig. 5: Counterexamples generated by FLEXIFAL using DTFAL algorithm.



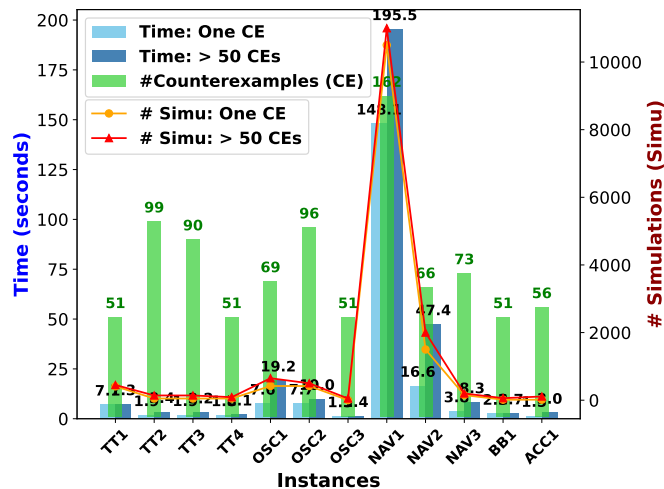


Fig. 6: #Simulations to find one vs multiple counterexamples nearly overlap. The time difference between finding one counterexample vs many is small in most of the instances.

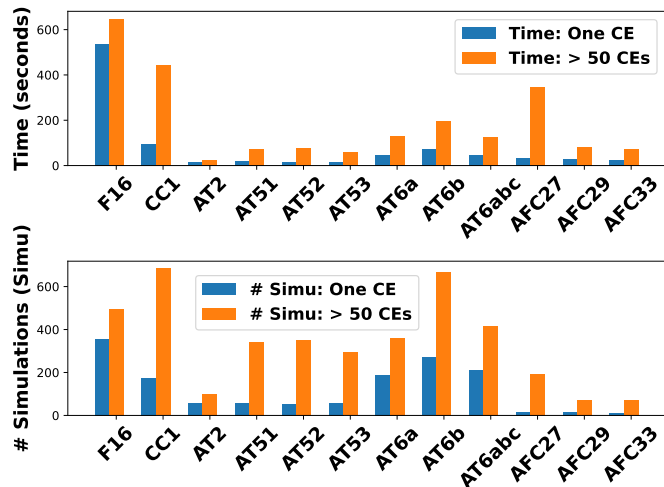


Fig. 7: Top: Time for finding 1 vs more than 50 counterexamples. Bottom: #simulations to find 1 vs more than 50 counterexamples across the Simulink instances.

D. RQ3: Generating multiple counterexamples efficiently

This section evaluates the ability of FLEXIFAL to generate multiple counterexamples efficiently. The NNFAL algorithm relies primarily on the DNN verifier or adversarial attack algorithms, which requires considerable computational effort just to obtain a single counterexample. Running the algorithm multiple times to find new counterexamples is expensive. In contrast, the DTFAL algorithm builds explanations for property violation, which can be potentially used to find multiple counterexamples with a little extra computational effort. The computational effort is measured by the number of random simulations and the time required to find them. Figures 6 and 7 show the results of finding many (> 50) counterexamples, and we see that DTFAL finds them with a little extra computational effort compared to finding just one.

Figure 7 shows the comparison for instances on Simulink

models. For example, DTFAL finds a single counterexample in F16 using 400 simulations in 513 seconds. In comparison, DTFAL generates 50 counterexamples using 500 simulations in 650 seconds, that is 49 more in less than 150 seconds with just 100 extra simulations.

VI. RELATED WORKS

Surrogate model-based CPS falsification: Recently, [28], [37] propose learning surrogate models from the CPS executions aiming to use them for falsification. A black-box technique with an approximation-refinement strategy is reported in [28] in which compute-intensive CPS that can take hours to simulate is converted to a surrogate model that is faster to execute. Surrogate models such as the Hammerstein-Wiener or the non-linear ARX model are generated using Matlab’s SI (System Identification) toolbox from the system’s input-output response. The surrogate is then tested against the specifications represented in signal temporal logic (STL). A falsifying trajectory is validated on the original CPS, and the surrogate model is iteratively refined to eliminate spurious trajectories. A robustness-guided black box checking for falsification of STL properties is reported in [37], in which a Mealy machine is constructed using automata learning. The counterexample in the Mealy machine is validated, and the model is refined to eliminate spurious counterexamples. FREAK [3] is a data-driven falsification tool that employs a surrogate model to replicate system dynamics. It uses Koopman operator linearization to construct a linear model of non-linear dynamics systems as a surrogate. The tool uses reachable analysis of the surrogate model and uses the reachability knowledge in the encoding of STL specifications into a Mixed-Integer Linear Program (MILP) to identify the least robust trajectory within the reachable state-space. If the trajectory is spurious, additional simulation data is generated to retrain the Koopman model and repeat the process until the instance is falsified. None of these works use machine learning models as CPS surrogates, which makes them different from our work.

Falsification tools for Simulink models: On the other hand, several state-of-the-art falsification tools for CPS represented as Simulink models are reported in [11], [9], [36], [28], [2], [37]. These algorithms are simulation-based falsification procedures for specifications written in Metric Temporal Logic (MTL) or Signal Temporal Logic (STL). A falsification algorithm proposed in [11] is based on adaptive Las-Vegas Tree Search (aLVTS), which constructs falsifying inputs incrementally in time. The fundamental concept is to start with simple inputs and scale up gradually by taking samples from input domains with improved temporal and spatial resolution. In [2], a toolbox is reported for falsifying MTL properties based on stochastic optimization techniques such as Monte-Carlo methods and Ant-Colony Optimization. The stochastic sampler suggests an input signal to the simulator which returns a trajectory. The robustness analyzer then examines the trajectory and returns a robustness value. The negative robustness value indicates that the toolbox falsifies the temporal property. A positive robustness value is used by the sampler to decide the next input. Ψ -TaLiRo [36] is another robustness-guided

falsification tool for CPS, which is a Python implementation of the toolbox proposed in [2]. The updated version supports built-in optimizers like DA and Uniform Random, with two new optimization algorithms such as Conjunctive Bayesian Optimization - Large Scale (ConBO-LS) and Part-X.

Breach [9] is a MATLAB toolbox mainly designed for STL specification monitoring and test case generation for hybrid dynamical systems. In addition, it supports optimization-based falsification and requirements mining for CPS. In contrary to these works, our falsification framework is data driven, making it application to any executable CPS in general and not limited to Simulink models per se.

Falsification tools for Hybrid Automaton Models: Hybrid automaton models of CPS have been studied with the focus on verification and model-checking. Some of the model-checkers for HA, such as DREACH [23], HYLAA [4], XSPEED [30], SAT-REACH [24]), have counterexample generation feature for reachability specifications expressed in their tool-specific language. As the computational effort in these tools is directed towards symbolic state-space exploration for proving safety rather than falsification, the computational effort that these tools incur for falsification is not comparable with falsification methods and tools. However, FLEXIFAL is capable of efficiently falsifying HA models with STL specifications.

VII. CONCLUSION

A data-driven framework has been proposed to falsify CPS safety specifications, which is primarily based on the building of a surrogate model, approximating a CPS given as an executable. The framework has the option to construct either a feedforward neural network or a decision tree as a surrogate model. The network-based falsification algorithm leverages *adversarial attack* algorithms and efficient verification tools for the falsification of reachability specifications. The use of a decision tree as a surrogate model has shown great promise on the falsification of CPS. The experimental evaluation indicates that our framework FLEXIFAL finds multiple hard-to-find counterexamples in CPS. The datasets and network surrogates of CPS have been made available in the public domain, which can be useful for novel machine learning-based analysis algorithms for CPS.

REFERENCES

- [1] Rajeev Alur, Costas Courcoubetis, Thomas A. Henzinger, and Pei-Hsin Ho. Hybrid automata: An algorithmic approach to the specification and verification of hybrid systems. pages 209–229. Springer-Verlag, 1992.
- [2] Yashwanth Annpureddy, Che Liu, Georgios Fainekos, and Sriram Sankaranarayanan. S-talro: A tool for temporal logic falsification for hybrid systems. In *TACAS 2011, Saarbrücken, Germany, March 26–April 3, 2011.*, pages 254–257. Springer, 2011.
- [3] Stanley Bak, Sergiy Bogomolov, Abdelrahman Hekal, Niklas Kochdumper, Ethan Lew, Andrew Mata, and Amir Rahmati. Falsification using reachability of surrogate koopman models. In *HSCC 24*, pages 1–13, 2024.
- [4] Stanley Bak and Parasara Sridhar Duggirala. Hylaa: A tool for computing simulation-equivalent reachability for linear systems. In *HSCC, Pittsburgh, PA, USA, April 18–20, 2017*, pages 173–178. ACM, 2017.
- [5] Stanley Bak, Hoang-Dung Tran, Kerianne Hobbs, and Taylor T Johnson. Improved geometric path enumeration for verifying relu neural networks. In *CAV 2020, Los Angeles, CA, USA, July 21–24, 2020*, pages 66–96. Springer, 2020.
- [6] Leo Breiman. *Classification and regression trees*. Routledge, 2017.
- [7] Lei Bu, Alessandro Abate, Dieky Adzkiya, Muhammad Syifa’ul Mufid, Rajarshi Ray, Yuming Wu, and Enea Zaffanella. ARCH-COMP20 category report: Hybrid systems with piecewise constant dynamics and bounded model checking. In *ARCH 2020.*, volume 74 of *EPiC Series in Computing*, pages 1–15. EasyChair, 2020.
- [8] Nicholas Carlini and David A. Wagner. Towards evaluating the robustness of neural networks. In *2017 IEEE Symposium on Security and Privacy, SP 2017, San Jose, CA, USA, May 22–26, 2017*, pages 39–57. IEEE Computer Society, 2017.
- [9] Alexandre Donzé. Breach, a toolbox for verification and parameter synthesis of hybrid systems. In *CAV 2010, Edinburgh, UK, July 15–19, 2010. Proceedings 22*, pages 167–170. Springer, 2010.
- [10] Alexandre Donzé and Oded Maler. Robust satisfaction of temporal logic over real-valued signals. In Krishnendu Chatterjee and Thomas A. Henzinger, editors, *Formal Modeling and Analysis of Timed Systems*, pages 92–106. Berlin, Heidelberg, 2010. Springer Berlin Heidelberg.
- [11] Gidon Ernst, Sean Sedwards, Zhenya Zhang, and Ichiro Hasuo. Fast falsification of hybrid systems using probabilistically adaptive input. In *QEST 2019, Glasgow, UK, September 10–12, 2019, Proceedings 16*, pages 165–181. Springer, 2019.
- [12] Chuchu Fan, Bolun Qi, Sayan Mitra, and Mahesh Viswanathan. Dryvr: Data-driven verification and compositional reasoning for automotive systems. In *CAV 2017, Heidelberg, Germany, July 24–28, 2017, Proceedings, Part I*, volume 10426, pages 441–461. Springer, 2017.
- [13] Ansgar Fehnker and Franjo Ivancic. Benchmarks for hybrid systems verification. In *HSCC*, pages 326–341, 2004.
- [14] Goran Frehse, Colas Le Guernic, Alexandre Donzé, Scott Cotton, Rajarshi Ray, Olivier Lebeltel, Rodolfo Ripado, Antoine Girard, Thao Dang, and Oded Maler. SpaceEx: Scalable Verification of Hybrid Systems. In *CAV, LNCS*. Springer, 2011.
- [15] Ian J Goodfellow, Jonathon Shlens, and Christian Szegedy. Explaining and harnessing adversarial examples. *arXiv preprint arXiv:1412.6572*, 2014.
- [16] Peter Heidlaufer, Alexander Collins, Michael Bolender, and Stanley Bak. Verification challenges in F-16 ground collision avoidance and other automated maneuvers. In *ARCH@ADHS 2018, Oxford, UK, July 13, 2018*, volume 54, pages 208–217. EasyChair, 2018.
- [17] Ian A. Hiskens. Stability of limit cycles in hybrid systems. In *34th Annual Hawaii International Conference on System Sciences (HICSS-34), January 3–6, 2001, Maui, Hawaii, USA*. IEEE Computer Society, 2001.
- [18] Bardh Hoxha, Houssam Abbas, and Georgios Fainekos. Benchmarks for temporal logic requirements for automotive systems. In *ARCH@CPSWeek 2014, Berlin, Germany, April 14, 2014 / ARCH@CPSWeek 2015, Seattle, WA, USA, April 13, 2015*, volume 34, pages 25–30. EasyChair, 2014.
- [19] Jianghai Hu, John Lygeros, and Shankar Sastry. Towards a theory of stochastic hybrid systems. In *HSCC 2000*, page 160–173. Berlin, Heidelberg, 2000. Springer-Verlag.
- [20] Xiaoqing Jin, Jyotirmoy V Deshmukh, James Kapinski, Koichi Ueda, and Ken Butts. Powertrain control verification benchmark. In *Proceedings of the 17th international conference on Hybrid systems: computation and control*, pages 253–262, 2014.
- [21] Guy Katz, Clark Barrett, David L Dill, Kyle Julian, and Mykel J Kochenderfer. Reluplex: An efficient smt solver for verifying deep neural networks. In *CAV 2017, Heidelberg, Germany, July 24–28, 2017, Proceedings, Part I 30*, pages 97–117. Springer, 2017.
- [22] Tanmay Khandait, Federico Formica, Paolo Arcaini, Surdeep Chotaliya, Georgios Fainekos, Abdelrahman Hekal, Atanu Kundu, Ethan Lew, Michele Loreti, Claudio Menghi, et al. Arch-comp 2024 category report: Falsification. In *Proceedings of the 11th Int. Workshop on Applied*, volume 103, pages 122–144, 2024.
- [23] Soonho Kong, Sicun Gao, Wei Chen, and Edmund Clarke. dreach: δ -reachability analysis for hybrid systems. In *TACAS 2015, London, UK, April 11–18, 2015, Proceedings*, volume 9035, page 200. Springer, 2015.
- [24] Atanu Kundu, Sarthak Das, and Rajarshi Ray. Sat-reach: A bounded model checker for affine hybrid systems. *ACM Trans. Embed. Comput. Syst.*, 22(2), jan 2023.
- [25] Alexey Kurakin, Ian J. Goodfellow, and Samy Bengio. Adversarial examples in the physical world. In *5th International Conference on Learning Representations, ICLR 2017, Toulon, France, April 24–26, 2017, Workshop Track Proceedings*. OpenReview.net, 2017.
- [26] Aleksander Madry, Aleksandar Makelov, Ludwig Schmidt, Dimitris Tsipras, and Adrian Vladu. Towards deep learning models resistant to adversarial attacks. *arXiv preprint arXiv:1706.06083*, 2017.

- [27] Oded Maler and Dejan Nickovic. Monitoring temporal properties of continuous signals. In *International Symposium on Formal Techniques in Real-Time and Fault-Tolerant Systems*, pages 152–166. Springer, 2004.
- [28] Claudio Menghi, Shiva Nejati, Lionel C. Briand, and Yago Isasi Parache. Approximation-refinement testing of compute-intensive cyber-physical models: an approach based on system identification. In Gregg Rothermel and Doo-Hwan Bae, editors, *ICSE '20, Seoul, South Korea, 27 June - 19 July, 2020*, pages 372–384. ACM, 2020.
- [29] Seyed-Mohsen Moosavi-Dezfooli, Alhussein Fawzi, and Pascal Frossard. Deepfool: A simple and accurate method to fool deep neural networks. In *CVPR 2016, Las Vegas, NV, USA, June 27-30*, pages 2574–2582. IEEE Computer Society, 2016.
- [30] Rajarshi Ray, Amit Gurung, Binayak Das, Ezio Bartocci, Sergiy Bogomolov, and Radu Grosu. XSpeed: Accelerating Reachability Analysis on Multi-core Processors. In *HVC 2015, Haifa, Israel, November 17-19, Proceedings*, pages 3–18, 2015.
- [31] Jérôme Rony, Luiz G Hafemann, Luiz S Oliveira, Ismail Ben Ayed, Robert Sabourin, and Eric Granger. Decoupling direction and norm for efficient gradient-based l2 adversarial attacks and defenses. In *Proceedings of the IEEE/CVF Conference on Computer Vision and Pattern Recognition*, pages 4322–4330, 2019.
- [32] Radu Serban and Alan C Hindmarsh. Cvodes: the sensitivity-enabled ode solver in sundials. In *International Design Engineering Technical Conferences and Computers and Information in Engineering Conference*, volume 47438, pages 257–269, 2005.
- [33] David Shriver, Sebastian Elbaum, and Matthew B Dwyer. Reducing dnn properties to enable falsification with adversarial attacks. In *2021 IEEE/ACM 43rd International Conference on Software Engineering (ICSE)*, pages 275–287. IEEE, 2021.
- [34] David Shriver, Sebastian G. Elbaum, and Matthew B. Dwyer. DNNV: A framework for deep neural network verification. In *CAV 2021, July 20-23, Proceedings, Part I*, volume 12759, pages 137–150. Springer, 2021.
- [35] Christian Szegedy, Wojciech Zaremba, Ilya Sutskever, Joan Bruna, Dumitru Erhan, Ian J. Goodfellow, and Rob Fergus. Intriguing properties of neural networks. In *ICLR 2014, Banff, AB, Canada, April 14-16, Conference Track Proceedings*, 2014.
- [36] Quinn Thibeault, Jacob Anderson, Aniruddh Chandratre, Giulia Pedrielli, and Georgios Fainekos. Psy-taliro: A python toolbox for search-based test generation for cyber-physical systems. In *FMICS 2021, Paris, France, August 24-26, Proceedings*, volume 12863, pages 223–231. Springer, 2021.
- [37] Masaki Waga. Falsification of cyber-physical systems with robustness-guided black-box checking. In *Proceedings of HSCC 23*, pages 1–13, 2020.
- [38] Shiqi Wang, Kexin Pei, Justin Whitehouse, Junfeng Yang, and Suman Jana. Efficient formal safety analysis of neural networks. *Advances in neural information processing systems*, 31, 2018.
- [39] Yipei Yan, Deyun Lyu, Zhenya Zhang, Paolo Arcaini, and Jianjun Zhao. Automated generation of benchmarks for falsification of stl specifications. *IEEE Transactions on Computer-Aided Design of Integrated Circuits and Systems*, 2025.
- [40] Xiaoyong Yuan, Pan He, Qile Zhu, and Xiaolin Li. Adversarial examples: Attacks and defenses for deep learning. *IEEE transactions on neural networks and learning systems*, 30(9):2805–2824, 2019.